



Process modelling and optimization of a 250 MW IGCC system: Model setup, validation, and preliminary predictions

Qilong Xu^a, Shuai Wang^{a,*}, Kun Luo^{a,b,**}, Yanfei Mu^a, Lu Pan^a, Jianren Fan^{a,b}

^a State Key Laboratory of Clean Energy Utilization, Zhejiang University, Hangzhou, 310027, China

^b Shanghai Institute for Advanced Study of Zhejiang University, Shanghai, 200120, China

ARTICLE INFO

Handling Editor: L Luo

Keywords:

IGCC
Process modelling
Power generation
Energy analysis
Exergy analysis

ABSTRACT

Integrated gasification combined cycle (IGCC) has emerged as a clean and efficient power generation technology, yet a cost-effective tool for process modelling and optimization of industrial-scale IGCC systems is still lacking. Accordingly, this work established an integrated model to predict the efficiency of a 250 MW industrial-scale IGCC system. After comprehensive validations with the design values and experimental data, the integrated model was used to predict power generation of the IGCC system under different load conditions (i.e., 50%, 70%, and 100%), with a focus on the efficiency assessment by energy analysis and exergy analysis. The results show that the IGCC system can operate stably under wide load conditions. Under the full load condition, the total power generation of the IGCC system is 262,051 kW; The thermal efficiency of the investigated IGCC system is 45.7%, higher than the conventional IGCC systems with energy efficiency in the range of 40%–45%. The exergy analysis considering the energy quality is more reasonable to assess the efficiency of the IGCC system with energy conversion and utilization, with an exergy efficiency of 41.8%. The air separation and gasification units have high energy consumption but low efficiency, which needs to be further optimized to improve system efficiency.

1. Introduction

Greenhouse gas emissions and energy depletion urge humans to seek clean and efficient energy utilization methods. At present, global fossil energy accounts for 80% of the total energy consumption, of which coal accounts for about 24% [1]. Coal has been long used as the main source of energy for human production activities for centuries due to its advantages of abundant reserves, low cost, and global distribution. One of the most used utilization methods for coal is thermoelectricity power generation, accounting for 31% of total power generation by 2030 [2]. However, coal as a non-renewable fossil fuel will produce greenhouse gas emissions (e.g., CO₂) and gas pollutants (e.g., SO₂ and NO_x) during the thermochemical conversion. Recently, two types of clean coal utilization technologies have emerged in the world [3]: (i) conventional coal-fired power plants by optimizing coal combustion modes, such as supercritical combustion technology, ultra-supercritical combustion technology [4,5], and circulating fluidized bed technology; (ii) integrated gasification combined cycle (IGCC) power plants by high-efficiency utilization of syngas from coal gasification for power generation [6].

Specifically, the IGCC technology uses a high-pressure gasifier to convert coal into pressurized syngas, which can then remove impurities from the syngas before the electricity generation cycle. Some of the pollutants can be turned into reusable byproducts through the Claus process, leading to lower emissions of SO_x, particulates, and in some cases CO₂. With additional process equipment, a water-gas shift reaction can increase gasification efficiency and reduce CO emissions by converting it to CO₂. The resulting CO₂ from the shift reaction can be separated, compressed, and stored through sequestration. Excess heat from the primary combustion and syngas-fired generation is then passed to a steam cycle, e.g., a gas turbine combined cycle. This process results in improved thermodynamic efficiency as compared to conventional pulverized coal combustion. According to the literature, the IGCC power plant featuring pulverized coal gasification to produce syngas and waste heat boilers to recover waste gas heat gives a thermal efficiency of 42% [7], higher than the conventional power plant [8]. Besides, the pollutant emissions from the IGCC power plant are 10% of the conventional power plants [9]. Thus, the IGCC technology provides a better way for clean and efficient utilization of coal by balancing power generation efficiency and gas pollutant emissions [10,11].

* Corresponding author.

** Corresponding author. State Key Laboratory of Clean Energy Utilization, Zhejiang University, Hangzhou, 310027, China.

E-mail addresses: wshuai2014@zju.edu.cn (S. Wang), zjulk@zju.edu.cn (K. Luo).

<https://doi.org/10.1016/j.energy.2023.127040>

Received 6 December 2022; Received in revised form 8 February 2023; Accepted 22 February 2023

Available online 9 March 2023

0360-5442/© 2023 Elsevier Ltd. All rights reserved.

Recently, people have struggled with the commercialization of IGCC technology, and the bottleneck lies in the higher investment costs and higher operating costs than the conventional coal-fired power plant [12]. Although the IGCC system uses a combined gas-steam cycle that increases the thermal efficiency to 42%, the power consumption of the air separation unit accounts for 17%–20% of the system power generation [13]. Currently, the Tianjin IGCC power plant consumes 400 g/kWh of pulverized coal for power generation, which is much higher than the supercritical coal-fired power plant with a coal consumption of 270 g/kWh. Therefore, it is necessary to reduce the overall energy consumption of the IGCC system and improve its overall economic efficiency. However, it is impractical to optimize the IGCC system through experiments via numerous trials and errors. In contrast, numerical simulation provides a cost-effective, repeatable, reasonable way for in-furnace phenomena investigation or process control/optimization of the IGCC system.

Currently, there are two main approaches for modelling the IGCC system: (i) computational fluid dynamics (CFD) simulation by solving the governing equations of the gas and solid phases, with a capacity of unveiling in-furnace phenomena, e.g., flow dynamics, heat and mass transfer, chemical reactions [29–31]; (ii) process simulation by solving heat and mass transfer balance formula under the equilibrium operating condition, with a capacity of aiding design and optimization [14]. On the one hand, the CFD simulation of flow dynamics or thermochemical properties inside each unit of the IGCC system (e.g., gasifier, turbine, heat recovery boiler) is unaffordable and unnecessary for system optimization. On the other hand, the CFD simulation concentrates on every single unit only and neglects the intrinsic interconnection between different units. In contrast, the process simulation circumvents the above drawbacks and provides a cost-effective way to model the whole IGCC system for process control and optimization.

Increasing attention has been paid to the process modelling and optimization of the IGCC system. For example, Lee et al. [15] used Pro/II software to examine the net power and energy loss of two exceptional grades of coal in the IGCC system and conducted a financial evaluation for each to decide the best economically efficient coal type. Ahmed et al. [16] developed an IGCC model coupled with carbon capture storage (CCS) and an IGCC system model integrated with a steam methane reforming reaction (SMR). After comparing the cost-effectiveness of the two systems, they found that the IGCC system integrated with SMR is more efficient, with reduced CO₂ emissions. Oh et al. [17] compared the efficiency and power prices of four different coals for a 500 MW IGCC system to evaluate the techno-economic and environmental costs of coal types. They demonstrated that the use of coals with a high moisture content results in higher energy consumption, worse cold gas efficiency, and higher economic costs. Giuffrida et al. [18] presented a complete IGCC power plant based on an air-brown gasifier and evaluated its thermodynamic performance. The overall performance of the plant was found to be improved with the air-blowing technology, with a calculated net efficiency increase of more than 1.5%. Additionally, they discussed the Sankey diagram of energy flow and the second law analysis for better energy analysis of the system. Xu et al. [19] proposed an IGCC system based on fuzzy supervisory predictive control (FSPC) according to the characteristics of IGCC power plants, and developed a combined energy and exergy optimization model from the laws of thermodynamics to calculate the energy efficiency and exergy efficiency to improve energy utilization efficiency and economic benefits. Wu et al. [20] conducted a process simulation for municipal solid waste, proposed an IGCC system for municipal solid waste based on energy analysis and exergy analysis, and compared energy efficiency and carbon emissions for three different designs to determine the best IGCC system. Lu et al. [21] constructed an IGCC plant that combined the sorption-enhanced water gas shift reaction process (SEWGS) with CO₂ removal. By performing process simulations using seven types of sorbents, they identified the best sorbents and the optimal temperature window for maximizing the thermal efficiency of the SEWGS-type IGCC plant. The IGCC system is composed of

several sub-systems, e.g., air separation unit, coal gasification and purification unit, and gas-steam combined cycle unit, and the previous studies are mainly focused on the process modelling and optimization of the whole system but neglect the interactions between the individual components. Moreover, they mainly focused on optimizing the IGCC system without comprehensive validations from the sub-system level to the overall system level.

To fulfill the above knowledge gap, this work established an integrated model to predict the efficiency of a 250 MW industrial-scale IGCC power plant from China Huaneng Group Co., Ltd. After comprehensive validations with the design values and experimental data, the integrated model was used to predict power generation of the IGCC system under different load conditions (i.e., 50%, 70%, and 100%), with a focus on the efficiency assessment by energy analysis and exergy analysis. The article is organized as follows: Section 2 gives the model establishment for IGCC sub-systems and model encapsulation of the IGCC system. Section 3 gives the power generation prediction of the designed IGCC system, with a subsequent thermodynamic analysis from the energy and exergy perspectives. The conclusion is drawn in the final section.

2. IGCC system model

2.1. Schematic of the IGCC system

IGCC is a next-generation thermal power system that combines coal gasification technology with a gas-steam combined cycle system, converting coal into pressurized gas (i.e., syngas), removing pollutants (e.g., sulphur) from the syngas through the desulfurization process, and finally transporting the purified syngas into the gas-steam turbine for electricity generation [11]. Fig. 1 shows the schematic of a typical IGCC system, which mainly includes three parts: an air separation unit (ASU), a coal gasification and purification unit, and a gas-steam combined cycle unit.

ASU aims to produce 99.6% oxygen and 99.9% nitrogen to supply the IGCC system for subsequent reactions. In industrial practice, the ASU commonly uses an air separation method to generate high-quality oxygen. The coal gasification unit and gas-steam turbine unit are the key parts of the IGCC system [22]. The former is mainly used to convert pulverized coal into syngas and purify the syngas subsequently. As the coal material contains a large amount of ash, sulphur, alkali metal salts and tar, the raw syngas produced from gasification needs to be purified by desulfurization and dust removal processes. The clean syngas is finally supplied to the gas-steam combined cycle unit – a unit consisting of gas turbines, heat recovery boilers (HRSG), steam turbines and other equipment, to convert chemical energy into electrical energy. The flue gas from the gas turbine has a high temperature of about 500–600 °C, and the HRSG is used to recover the heat from the flue gas in multiple stages. The gas-steam combined cycle combines the Brayton cycle of the gas turbine and the Rankine cycle of the steam turbine, fully realizing the cascade utilization of energy. The structure and operating conditions of the gas-steam combined cycle unit directly determine the thermal efficiency of the IGCC system.

2.2. Model establishment for IGCC sub-systems

2.2.1. Air separation unit

This section shows the establishment of the ASU model on the Aspen Plus and the subsequent validation with the design values of a 250 MW IGCC power plant from China Huaneng Group Co., Ltd. Specifically, air filters and air adsorbers are neglected in the air separation process of the ASU model due to their weak pressure variations and insignificant effects on energy consumption. The air fed to the air compressor is assumed to be impurity-free air (i.e., 78.118% N₂, 20.95% O₂, and 0.932% Ar). Oxygen with a total flow rate of 46,000 Nm³/h is required for the subsequent gasification process. Thus, the air required can be evaluated by the material balance equation using a simplified binary

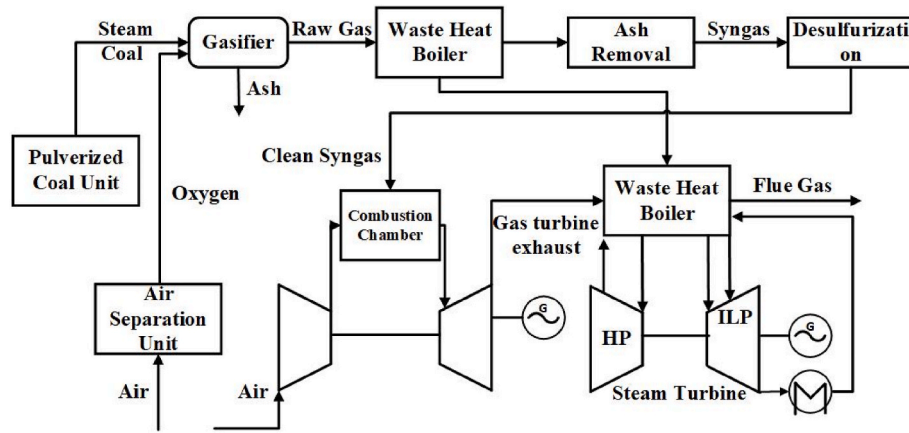


Fig. 1. Schematic of the IGCC system.

system with 99.6% oxygen and 99.9% nitrogen:

$$V_A = V_O + V_N \quad (1)$$

$$V_A P_{AN} = V_O P_{ON} + V_N P_{NN} \quad (2)$$

where V_A , V_O , and V_N are the volume of raw air, oxygen product, and nitrogen product, respectively. P_{AN} , P_{ON} , and P_{NN} are the molar fraction of nitrogen in air, oxygen product, and nitrogen product, respectively. The above equations correspond to 1.0 Nm^3 of air. Thus, the theoretical production of oxygen is formulated by:

$$V_A = V_O \times \frac{P_{ON} - P_{NN}}{P_{AN} - P_{NN}} = V_A \times \frac{0.4\% - 99.99\%}{79.1\% - 99.99\%} = 4.767V_O \quad (3)$$

Accordingly, at least 219,282 Nm^3/h of raw air is theoretically required for producing 46,000 Nm^3/h of oxygen. A loss factor of the system with 0.86 is introduced to consider gas dissipation and leakage. Ultimately, 253,000 Nm^3/h of air is required for the ASU. Fig. 2 shows the schematic of the ASU model. The air compressor and multi-stage compressor are centrifugal compressors with an isentropic efficiency of 0.8 at all stages. The main material parameters of the ASU are shown

in Table S1 of the supplementary material.

This ASU model is validated with the design values from a 250 MW IGCC power plant from China Huaneng Group Co., Ltd. The product yields and purity are represented in Fig. 3, it is noted that the predicted medium-pressure oxygen production is 46707.44 scmh and low-pressure nitrogen production is 20595.7 scmh, slightly higher than the design values. The relative errors are within 5%, meeting the design standard. The predicted purity of oxygen is 99.4% and the purity of nitrogen is 99.75%, slightly lower than the design values. The relative errors are within 1%, meeting the design standard. The discrepancies in the production of oxygen and nitrogen result from the neglect of gas losses such as pipeline leakage and protection gas in the AUS model. However, the slight discrepancies are acceptable, demonstrating the reasonability of the present model in predicting the ASU.

2.2.2. Coal gasification and purification unit

This section shows the establishment of the model for describing the coal gasification and purification unit. Specifically, coal, oxygen and steam are fed into the gasifier. Coal is burnt in oxygen conditions, and the generated carbon dioxide further reacts with steam to produce

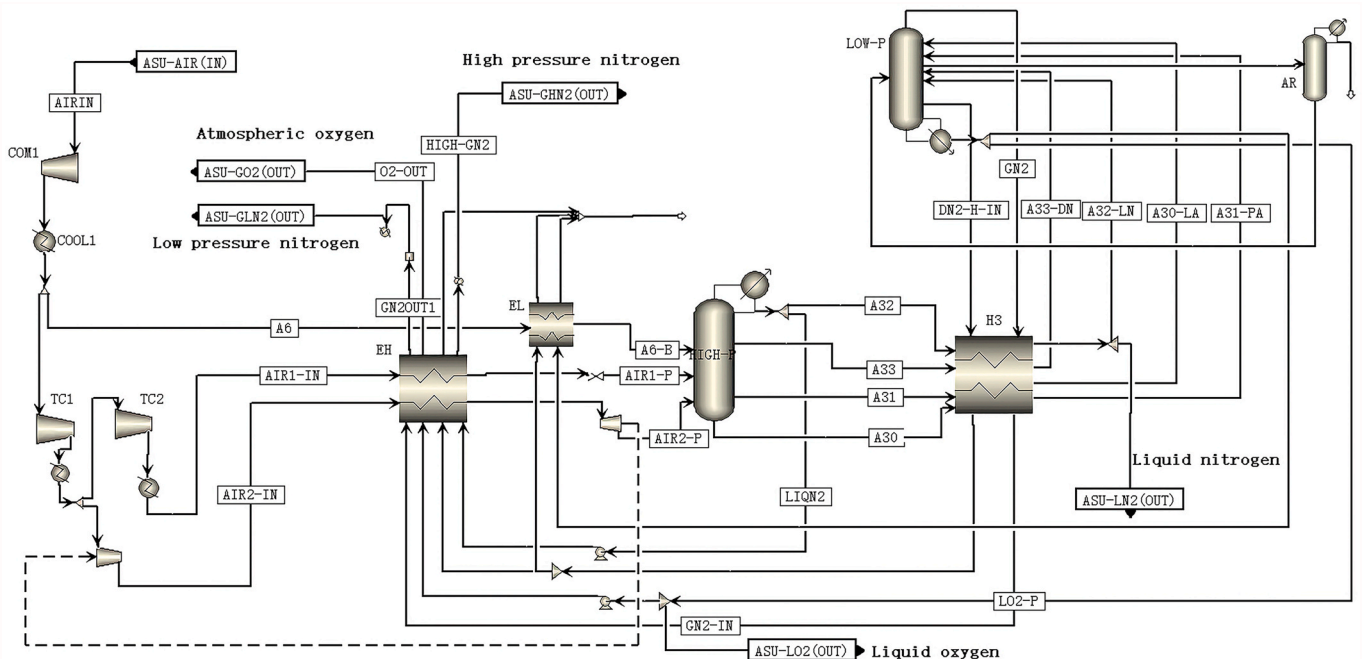


Fig. 2. Process modelling of the ASU.

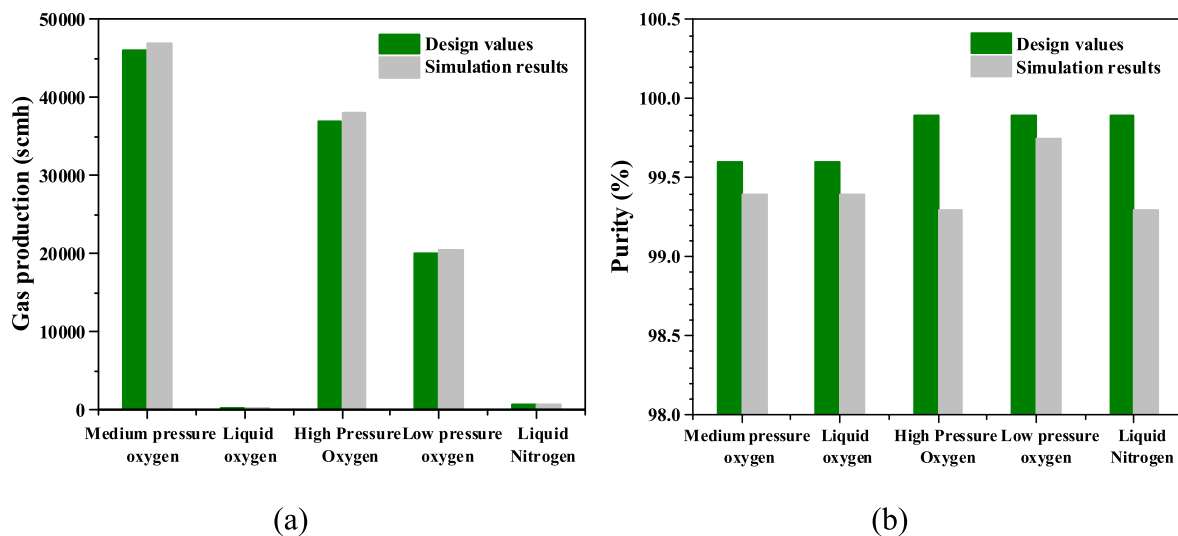


Fig. 3. Comparison of gas production (a) and purity (b) of the ASU between simulation results and design values.

carbon oxide and hydrogen. Table 1 lists the main reactions of coal gasification in the gasifier. Several assumptions are made in building the coal gasification and purification unit model as follows.

- The gasifier is in a steady state, under isothermal, adiabatic and thermodynamic equilibrium conditions. The feeding rate of coal material keeps constant.
- Pulverized coal particles are spherical and isothermal, without considering the formation, solidification, and discharge of slag in the gasifier.
- The mixing, pyrolysis, and gasification of pulverized coal are completed instantly in the gasifier.
- H, O, N, S and Cl in the pulverized coal are converted to the gas phase and the ash is discharged directly without participating in the reaction.
- The production of tar and other heavy hydrocarbons is ignored due to their insignificant amounts.

Fig. 4 shows the process modelling of the coal gasification and purification unit. Specifically, the reaction in the two-stage dry pulverized coal gasifier is divided into the coal combustion and gasification processes. The former generates high-temperature flue gas to enter the second stage using the BSTOI and BURN models. The gasification process produces syngas with their composition and temperature calculated by RSTOI and GASIFIC models. The SPLIT is a gas-solid separator, which separates the unburned carbon and ash in the flue gas. The heat of pyrolysis from BSTOI and GASSTOI and the heat of combustion from BURN are introduced into the GASIFIER to support the endothermic gasification reactions. A FSPLIT model is used for separators H₂O-FSP, N₂-FSP, and COAL-FSP, with a specific proportion for each separator. A SSPLIT model is employed for separator SPLIT1. A heater model is assigned for

Table 1

The main reactions of coal gasification in the gasifier.

| Reaction | Reaction name | Heat of reaction |
|---|----------------------------------|----------------------------------|
| $C + 0.5O_2 \rightarrow CO$ | Partial oxidation | $\Delta H = -111 \text{ kJ/mol}$ |
| $CO + 0.5O_2 \rightarrow CO_2$ | Complete oxidation | $\Delta H = -283 \text{ kJ/mol}$ |
| $H_2 + 0.5O_2 \rightarrow H_2O$ | Hydrogen combustion | $\Delta H = -242 \text{ kJ/mol}$ |
| $C + CO_2 \rightarrow 2CO$ | Boudouard reaction | $\Delta H = +172 \text{ kJ/mol}$ |
| $C + 2H_2 \leftrightarrow CH_4$ | Methanation reaction | $\Delta H = -75 \text{ kJ/mol}$ |
| $C + H_2O \leftrightarrow CO + H_2$ | Char reforming reaction | $\Delta H = +131 \text{ kJ/mol}$ |
| $CO + H_2O \leftrightarrow CO_2 + H_2$ | Water gas-shift reaction | $\Delta H = -41 \text{ kJ/mol}$ |
| $CH_4 + H_2O \leftrightarrow CO + 3H_2$ | Steam-methane reforming reaction | $\Delta H = +206 \text{ kJ/mol}$ |

the ash separation and slag cooler COOL. A SEP model is specified for the supplementary stream heat loss absorber SEP, aiming to absorb H₂S and CO₂ in syngas. Q1 and Q5 are the heat loss from pyrolysis and Q4 is the heat release from combustion. The heat exchanger COOL aims to cool the syngas and the SEP is the separator for H₂S and CO₂ separation to achieve desulfurization and carbon capture.

Shenhua coal is used in the gasification process, and its proximate and ultimate analysis is listed in Table 2. The lower heating value (LHV) is 22.215 MJ/kg. The feed parameters of the two-stage dry pulverized coal gasifier (e.g., pressure, temperature, first-stage mass flow rate, second-stage mass flow rate, and total flow rate) are summarized in Table S2 of the supplementary material. Specifically, the mass flow rates of pulverized coal for the first and second states are 20.988 kg/s and 3.2988 kg/s, respectively.

The model is validated with the experimental data regarding the molar fraction of syngas after the gasification process. As shown in Fig. 5, CO occupies the largest proportion about 65%, followed by H₂, N₂, CO₂, and CH₄. The molar fraction of gas pollutants such as COS and H₂S are tiny due to their small amounts initially in the coal material. The discrepancies between the simulation results and experimental data stem from the above-mentioned model assumptions. However, such slight discrepancies are acceptable in practical industries. Besides, the carbon conversion rate (i.e., defined as the ratio of carbon content of the syngas to that of the pulverized coal), gasification efficiency (i.e., defined as the ratio of the calorific value of syngas to the heat of combustion of coal), and outlet temperature predicted from the present simulation agree with the experimental data. Particularly, the carbon conversion ratio is one of the most important indicators of the operation of a gasifier, which is calculated based on the carbon content of the feed coal in the reaction, the coal conversion rate (normally set to 97% under ideal conditions) and the carbon content of the syngas at the end of the gasification reaction in the gasifier. These parameters agree well with the experimental data, with relative errors of 0.5%, 0.8%, and 3.0%, respectively (see Table 3). Thus, the present model is reliable to predict the coal gasification and purification unit.

2.2.3. Gas-steam combined cycle unit

Gas-steam combined cycle unit includes the gas turbine system and heat recovery steam generator (HRSG) system. In the gas turbine system, air compression, syngas combustion, and turbine work take place. Specifically, air enters from the compressor and then is compressed and heated up. 87% of the compressed air is sent to the combustion chamber to burn and the flue gas enters the gas turbine to do work. The rest of the compressed air enters the cooler to cool down and be introduced to the

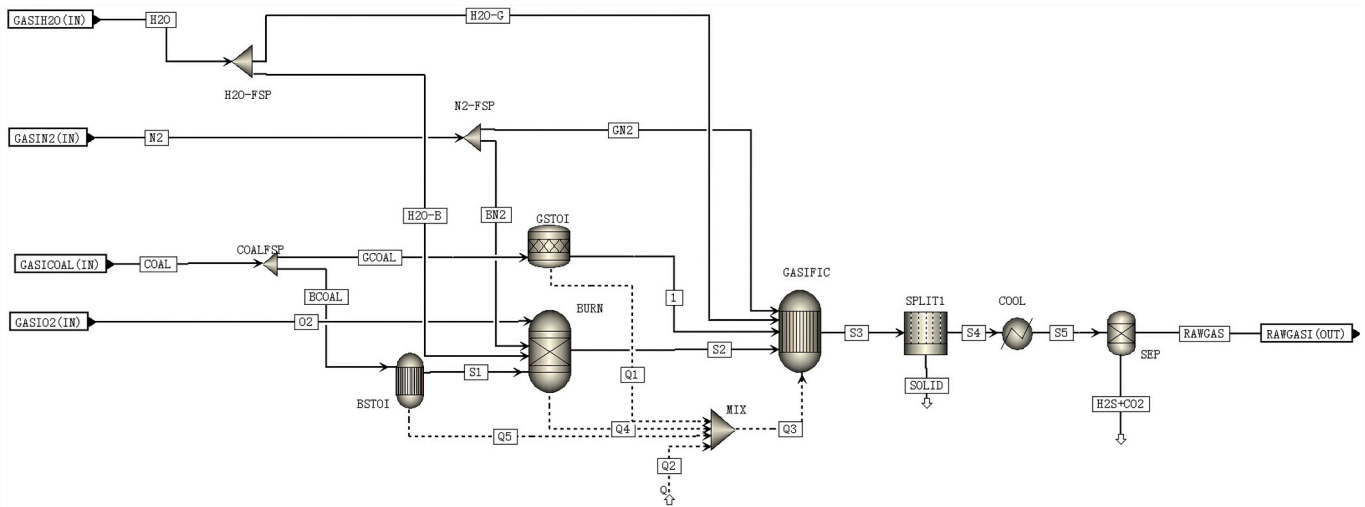


Fig. 4. Process modelling of the coal gasification and purification unit.

Table 2
Proximate and ultimate analysis of Shenhua coal.

| Ultimate analysis | Weight as received (%) | Proximate Analysis | Weight as received (%) |
|-------------------|------------------------|--------------------|------------------------|
| Carbon | 60.33 | Moisture | 14.00 |
| Hydrogen | 3.62 | Fixed Carbon | 47.67 |
| Oxygen | 9.95 | Volatiles | 27.33 |
| Nitrogen | 0.70 | Ash | 11.00 |
| Sulphur | 0.40 | | |

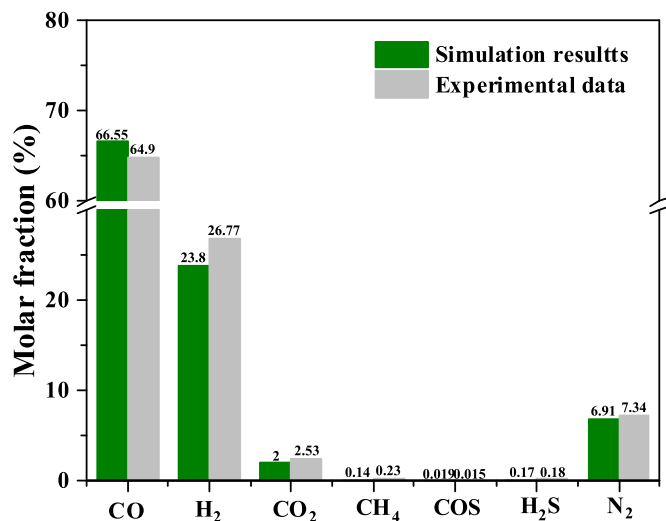


Fig. 5. Comparison of the predicted molar fraction of syngas with the experimental data.

Table 3
Comparison of predicted outputs with experimental data.

| | Carbon conversion rate (%) | Gasification efficiency (%) | Outlet temperature (K) |
|------------|----------------------------|-----------------------------|------------------------|
| Experiment | 98.5 | 83 | 1580 |
| Simulation | 98 | 83.67 | 1627.3 |

gas turbine. Fig. 6 shows the process modelling of the gas turbine unit, where the compressor, combustion chamber, turbine, and condenser are described by the AIR-TUR, COMBUSTI, TURBINE, and COOL models, respectively. The FSPLIT and MIXER models are used to denote the splitting and mixing of the flow. The MIX-W model accounts for the consumption power of the compressor and the output power of the gas turbine. The physical property method is chosen as PENG-ROB, which is suitable for non-polar or weakly polar mixed systems.

The HRSG unit consists of three systems, including 13 heat exchangers, 3 steam packages, and 3 turbines. The physical parameters of gas and solid phases are determined by the PENG-ROB and STEAM-TA methods. Specifically, the STEAM-TA method is established based on the ASME-1967 steam correlation, which is accurate to calculate the transition of steam-water-ice three phases. Fig. 7 shows the process modelling of the HRSG unit, where the heat exchanger, steam package, and steam turbine are denoted by the HeatX, Flash2, and Compr models. Besides, the steam turbine is realized by three compressors, including a low-pressure engine, a medium-pressure engine, and a high-pressure engine. Specifically, the incoming steam of the low-pressure engine (LP) is mainly pumped by the low-pressure superheater and the medium-pressure engine to do work; the steam from reheater 2 enters the medium-pressure engine (IP1) to do work; the incoming steam of the high-pressure engine (HPTURB) is mainly pumped by the high-pressure superheater 2. 1 W, 3 W, and 4 W refer to the work done by low-pressure, medium-pressure, and high-pressure engines, respectively. Flash2 model is adopted for the steam drum, where the steam and water are separated, with the steam escaping from the top and water draining from the bottom.

The model for the gas-steam combined cycle unit is validated with the experimental data. The isentropic efficiency of the air compressor and gas turbine is specified as 0.89, and the isentropic efficiencies of the low-pressure, medium-pressure, and high-pressure engines are set as 0.875. Table S3 of the supplementary material lists the inlet parameters. 215.36 kg/s syngas and 1405.8 kg/s air are introduced into the gas turbine to drive it to do work by combustion, with a power generation of 163,037 kW. With a temperature of about 569.23 °C, the flue gas from the gas turbine is introduced into the heat recovery boiler. The generated high-temperature steam is fed into the steam turbine to do work, which has a low-pressure engine, a medium-pressure engine, and a high-pressure engine.

The flue gas and water have an opposite trend by analyzing the parameters of the HRSG as listed in Table S4 of the Supplementary materials. Specifically, the water is gradually heated and gasified to the superheated state, which can generate 196.4t high-pressure superheated

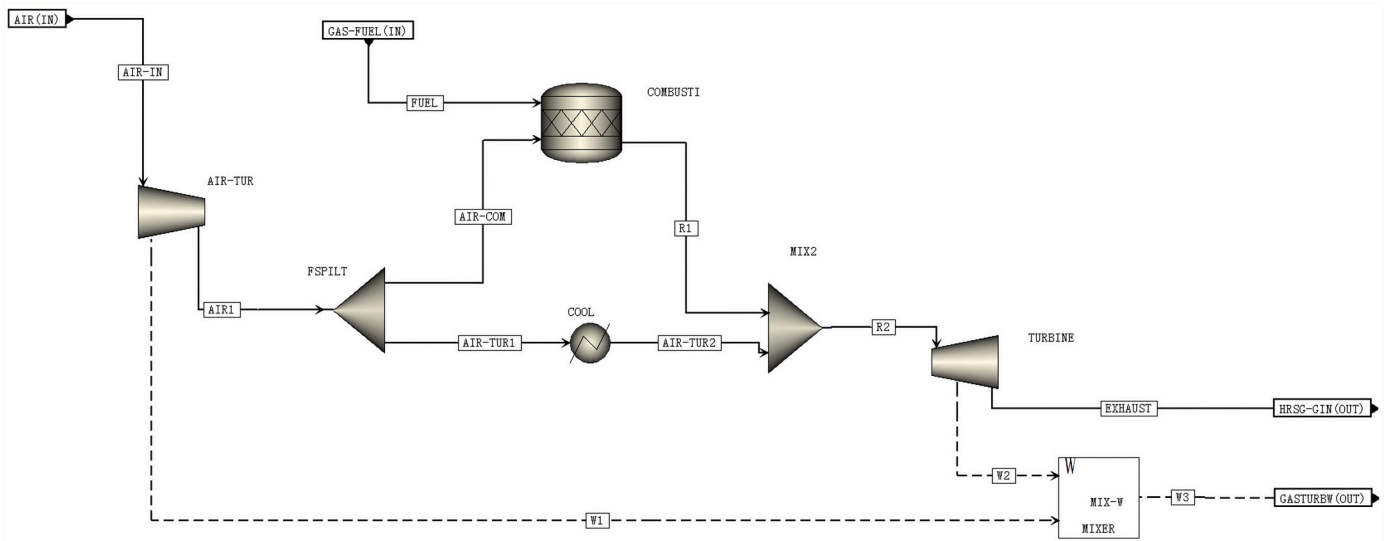


Fig. 6. Process modelling of the gas turbine unit.

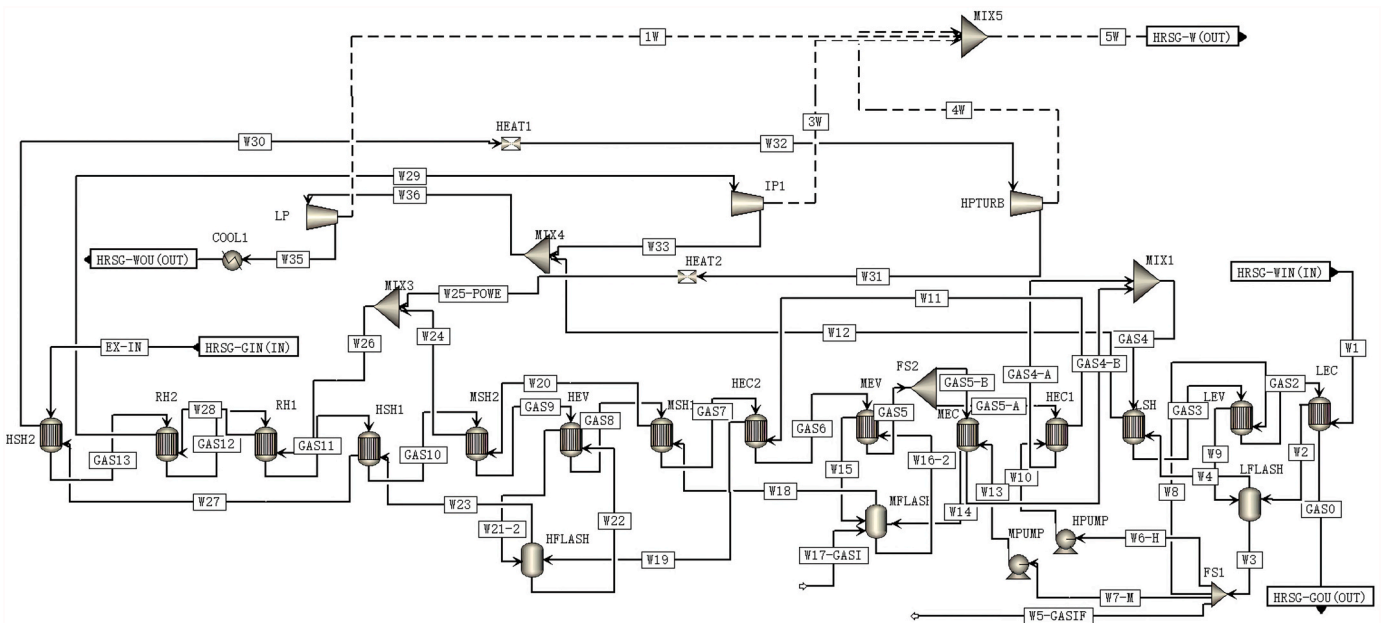


Fig. 7. Process simulation of the HRSG unit.

steam (92 bar, 521.9 °C), 74.1t medium-pressure superheated steam (44 bar, 293.6 °C), and 31.53t low-pressure saturated steam (5.92 bar, 207.2 °C). The flue gas reduces its temperature from 569.23 °C to 72.47 °C and is finally exhausted to the atmosphere. Working fluid keeps a fixed temperature in the low-pressure, medium-pressure, and high-pressure evaporators, but it will be partially evaporated by recovering the heat from flue gas. The existence of a heat recovery boiler can recover the heat from flue gas in cascades, which greatly improves the thermal efficiency of the overall system.

Table 4 compares the simulation results with the operation data obtained from the practical power plant. The simulation results of the gas turbine and HRSG units agree well with the experimental data, with acceptable relative errors. Specifically, the power generation from the gas turbine is slightly lower than the actual working condition because the amount of air and syngas in the model design is slightly lower than that in the actual operation. However, a relative error of about 5% is acceptable. Therefore, the model for the gas-steam combined cycle unit

Table 4

Comparison of the gas-steam combined cycle outputs between simulation results and experimental data.

| Parameters | Simulation result | Experimental data | Relative Error (%) |
|-------------------------------|-------------------|-------------------|--------------------|
| Air flow rate (kg/s) | 1405.8 | 1460 | 3.7 |
| Syngas flow rate (kg/s) | 215.6 | 220 | 2 |
| Turbine outlet temperature(K) | 842.2 | 827 | 1.8 |
| Exhaust temperature(K) | 345.5 | 345 | 0.15 |
| Gas turbine power (kW) | 163,436 | 172,000 | 4.8 |
| Steam turbine power (kW) | 90,179 | 92,560 | 2.6 |
| Gas turbine efficiency (%) | 33.57 | 34.87 | 3.7 |
| Heat efficiency (%) | 52.13 | 53.5 | 2.6 |

is reliable and can be used for subsequent process simulations.

2.3. Model encapsulation of the IGCC system

In this section, the above well-validated models for IGCC sub-systems are encapsulated into a whole IGCC system model. Specifically, the ASU adopts an independent air separation process, the coal gasification and purification unit adopts a two-stage dry pulverized coal gasifier and an ambient wet purification process, the gas turbine engine adopts a single-stage gas turbine, and the HRSG adopts a three-pressure cycle system. The ASU, coal gasification unit, gas turbine, and HRSG are encapsulated in turn, i.e., ASU, GASI, GASTURB and HRSG models form a complete IGCC system, as shown in Fig. 8. The heat exchangers, pressure transmitters, and shunts are used to combine each sub-system.

- 1) Air ASU-AIR enters the ASU to generate oxygen ASU-GO2 with 99.4% oxygen and is heated by heat exchanger HEAT-O2. The air is then introduced into the coal gasification purification unit GASI. Part of liquid nitrogen ASU-GLN2 is pressurized by compressor COMP-N2 into the GASI model to transport pulverized coal and stabilize temperature in the gasifier. Part of high-pressure nitrogen ASU-GHN2 is mixed with the syngas generated from the gasification unit to ensure that the calorific value of syngas is not too high. The other generated liquid oxygen and liquid nitrogen are stored by the TANK model.
- 2) For the coal gasification and purification unit GASI, a certain amount of pulverized coal GASICOAL and saturated steam are specified as inputs, and the gasification reaction with pure oxygen occurs to produce syngas RAWGASI. The syngas is then mixed with a small amount of steam and nitrogen, heated by heat exchanger HEAT-GAS, and passed to the gas turbine.
- 3) In the gas turbine GASTURB unit, the air reacts with syngas to do work, generating high-temperature flue gas HRSG-GIN. In the HRSG, heat exchange occurs between the high-temperature flue gas and water HRSG-WIN, and the resulting steam drives the turbine to do work. Workstream GASTURBW, HRSG-W, and W are the output work of the gas turbine, the output work of the combined cycle of the heat recovery boiler and turbine, and the total output work of the power island, respectively.

Table 5 lists the parameters of each inlet flow unit of the IGCC system, where 326.89 t/h of air, 81.7 t/h of Shenhua coal and 15 t/h of H₂O are fed into the system. The products generated by the ASU are shown in Table S5 of the Supplementary materials. The IGCC system runs at full load condition, and the parameters of the syngas produced after desulfurization and decarbonization are listed in Table S6 of the Supplementary materials.

In the HRSG, 1405.08 t/h of air is fed to the gasification unit and the syngas from the gasification unit undergoes a strong redox reaction. The

Table 5 Parameters of inlet flow units of the IGCC system.

| Stream | ASU | Gasification | | Syngas | Gas Turbine | HRSG |
|-----------------|-------|--------------|---------|---------|-------------|----------|
| | AIR1 | GASICOAL | GASIH2O | H2O-GAS | AIR | HRSG-WIN |
| T(K) | 26.5 | 80 | 573.15 | 263 | 12.6 | 262.1 |
| P (bar) | 1.015 | 40 | 50.5 | 48.5 | 1.01 | 45.09 |
| Mass flow (t/h) | 326.9 | 81.7 | 15 | 68 | 1405.8 | 49.1 |

high-temperature flue gas and 49.1 t/h of water enter the heat recovery boiler, and the heat exchange is distributed counter-currently. At the end of the cycle, the flue gas temperature is reduced to 376.65 K. In the combined cycle, the gas turbine and steam turbine do work, as shown in Table 6. The total power generated by the IGCC system in the full load condition is 262,051 kW after the action of ASU, coal gasification and purification unit, and gas-steam combined cycle unit.

3. Results and discussion

3.1. Power generation

The above IGCC system is mainly operated under the full load condition. However, the IGCC system is also operated under different load conditions according to industry practice, thus the IGCC model can be applied for process modelling under different load conditions. In the practical operation of the IGCC power plant, it is impractical to adjust (e.g., start-up, shut-down) the ASU and gasification units due to unaffordable time consumption. Accordingly, the adjustment parameters are simplified by keeping the parameters of the ASU and gasification units unchanged during the adjustment operation, but only adjusting the gas intake to the power island to achieve the goal. Specifically, four splitters are added as the regulation valves of gas flow based on the 100% full

Table 6 Power generation of the sub-systems and whole IGCC system.

| Air compressor power consumption (kW) | Gas turbine power generation (kW) | Steam turbine power generation (kW) | | | Total power generation (kW) |
|---------------------------------------|-----------------------------------|-------------------------------------|------------------------|----------------------|-----------------------------|
| | | Low-pressure engine | Medium pressure engine | High-pressure engine | |
| 128,670 | 291,706 | 53,588 | 34,788 | 10,640 | 262,052 |

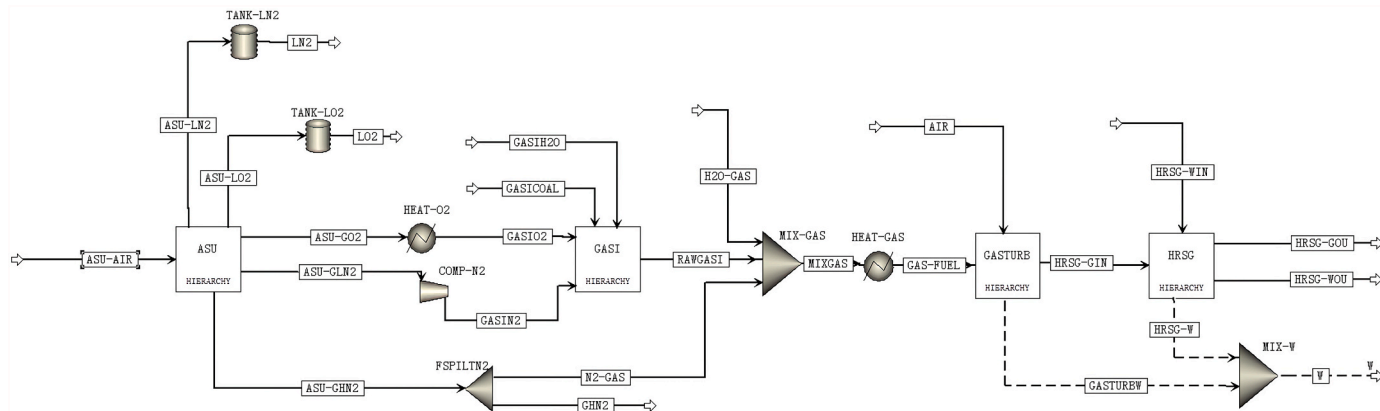


Fig. 8. Process modelling of the whole IGCC system.

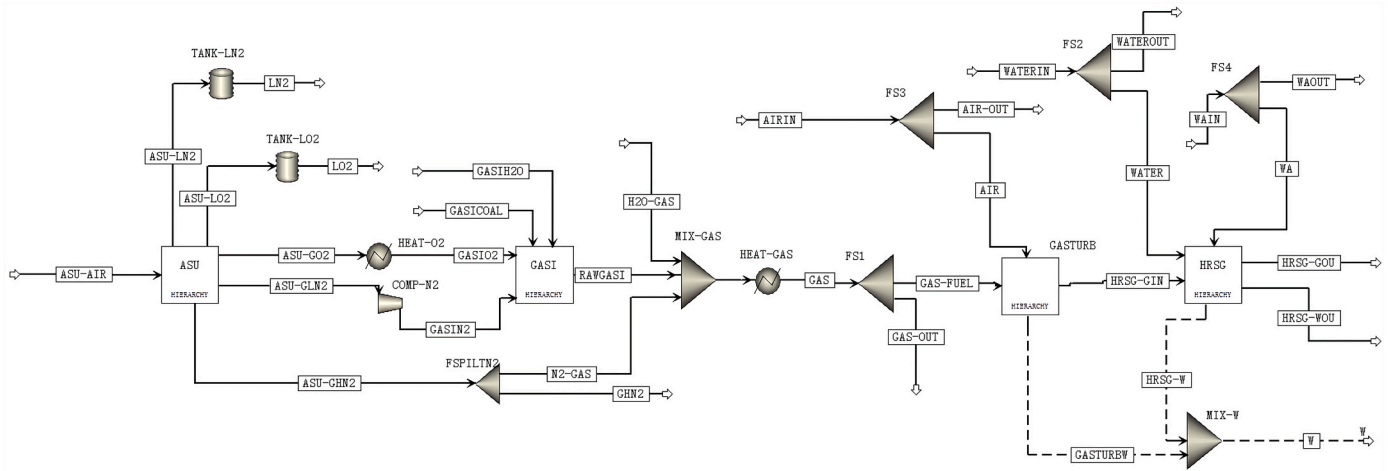


Fig. 9. Process modelling of the IGCC system under variable operating conditions.

load condition, as shown in Fig. 9. The process modelling of the IGCC system under variable load conditions is fulfilled, where the ASU and gasification unit are not modified.

Specifically, FS1 is the diverter of the syngas, FS2 is the inlet diverter of the heat recovery boiler, FS3 is the air diverter of the gas turbine, and FS4 is the supplemental water diverter of the heat recovery boiler. Different operating conditions are achieved by adjusting the splitters ratio of each splitter. Moreover, GAS-OUT is the syngas that does not flow into the subsequent gas-steam combined cycle, which will subsequently be used in areas such as the synthesis of liquid fuels. The present study is mainly focused on the analysis of the IGCC system, thus the utilization of syngas in other manners is not considered in this work. In addition, MIX-W allows for the generation of the two components of the gas-steam combined cycle, W, to be adjusted to the plant’s needs in real time, and design specifications are set for this generation to obtain the corresponding generation, which is based on the power generation required at each moment and is closely related to W. Through this process, an accurate simulation of the variable operating conditions of the IGCC system can be achieved by Aspen plus.

Fig. 10 shows the power generation of the gas-steam combined cycle unit under different load conditions (i.e., 50%, 70%, 100%). Increasing the load increases the amount of syngas generated and promotes the amount of work done. Specifically, increasing the load from 50% to 100%, the power consumption in the air compressor and power

generation in the gas turbine are promoted by 98.3% and 99.2%, respectively. The power generation of the total gas turbine system under 50%, 70%, and 100% loads is 81,530 kW, 114,320 kW, and 164,547 kW. Since the power generation by the gas turbine unit is calculated by subtracting the work consumed by the air compressor, the final total work will be less than the work done by the gas turbine. In the steam turbine unit, the low-pressure engine has the largest power generation under all load conditions, followed by the medium-pressure engine and high-pressure engine. For the low-pressure engine, the power generation increases by 93.5% from 50% load to 100% load; for the medium-pressure engine, the power generation increases by 92.5% from 50% load to 100% load; for the high-pressure engine, the power generation increases by 92.3% from 50% load to 100% load. Therefore, it can be concluded that the IGCC system can operate stably under different operating conditions.

Fig. 11 shows the power generation of each system and the total system under different load conditions. Specifically, by increasing the load from 50% to 100%, the power generation of the steam turbine and gas turbine increases by 93.1% and 99.9%, respectively. In addition, the total power generation of the IGCC system increases by 97.1%. Adjusting the syngas inlet can directly regulate the power island work situation, and finally, regulate the external work of the IGCC system. When the power plant encounters the peak regulation situation, clean gas storage tanks can be prepared to store the clean syngas for high-load

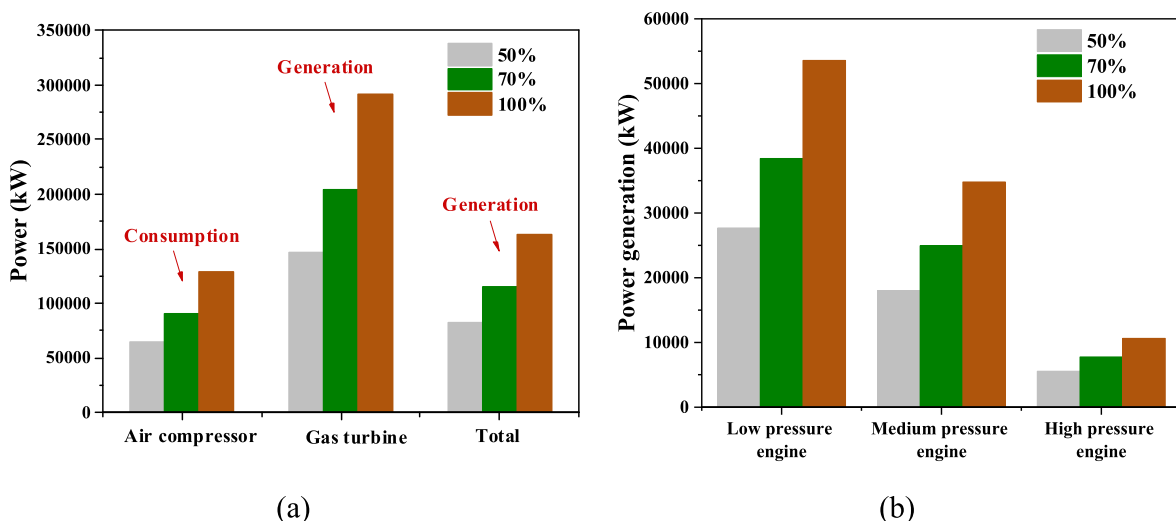


Fig. 10. Power generation under different load conditions: (a) gas turbine system and (b) steam turbine system.

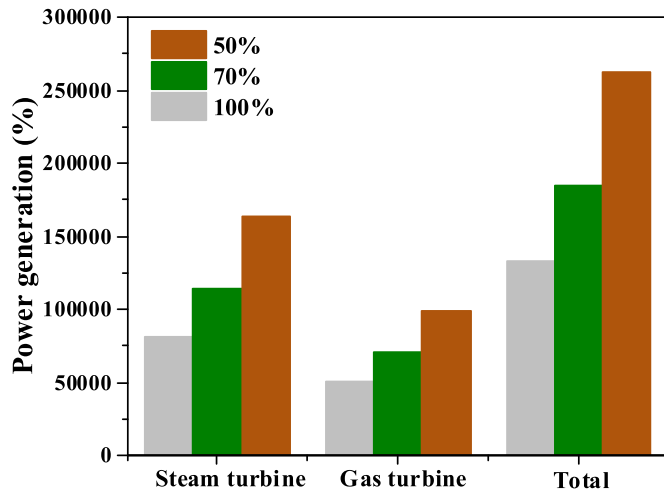


Fig. 11. Power generation of the IGCC system under different working conditions, including the power generation from the steam turbine system, gas turbine system, and the total IGCC system.

operation.

3.2. Thermodynamic analysis

To deeply analyze the performance of the IGCC system, thermodynamic analysis was also performed, including energy analysis and exergy analysis. In the thermodynamic analysis of the IGCC system, the variable operating conditions are more complex and the change in input energy after the change in different load conditions needs to be taken into account, but the overall energy change is similar to that of the 100% load condition, so the following thermodynamic analysis will be carried out for the 100% load condition.

3.2.1. Energy analysis

The energy analysis of IGCC systems is a mainstream method to examine the system's performance. It is based on the first law of thermodynamics to analyze the thermal efficiency of the system, which evaluates the energy system from the view of the quantitative utilization of energy and facilitates the quantitative analysis of the energy system. For a system in steady operation, its energy balance equation under controlled volume conditions can be expressed as [23]:

$$Q - W = \sum_{out} m_i h_i - \sum_{in} m_i h_i \quad (4)$$

where Q is the net heat flow rate of the sub-system; W is the work done by the system to the environment; m_i and h_i denote the mass flow rate and specific enthalpy of the streams, respectively. The energy efficiency of the subsystem can be expressed as:

$$\eta_i = \frac{E_{out,i}}{E_{in,i}} \times 100\% \quad (5)$$

where $E_{out,i}$ denotes the energy output by sub-system i . $E_{in,i}$ denotes the energy input by the sub-system i .

The net efficiency of the IGCC system is the ratio of net output power to the heat input of raw coal. The net output power is obtained by subtracting the plant consumption power from the total power generation, the sum of the power output of the gas turbine and the steam turbine is the total power generated by the system, and the plant consumption power includes the power consumed by the ASU and all auxiliary machines. Accordingly, the net efficiency of the IGCC system is calculated as [24]:

$$\eta_{th} = \frac{W_{net}}{M_{coal} \times LHV_{coal}} \times 100\% \quad (6)$$

where W_{net} is the net power output, which is the sum of the net power output of the gas turbine, the power output of the steam turbine, and the auxiliary power consumption of the pump and compressor. M_{coal} is the mass flow rate of the coal. LHV_{coal} is the low heat value of coal.

The energy efficiency of the ASU, gasification unit, gas turbine unit and HSRG unit are 10.9%, 61.2%, 94.7%, and 93.2%, respectively. The thermal efficiency of the IGCC system is 45.7%.

3.2.2. Exergy analysis

Although the energy analysis described above allows quantitative analysis of IGCC systems, it does not involve the assessment of energy quality in the analysis process. If only thermal efficiency is used as the evaluation criterion, it is insufficient to accurately evaluate the system performance [25]. In contrast, exergy analysis is based on the first law of thermodynamics and the second law of thermodynamics, which integrates the quantity and quality of energy and can evaluate the energy system more scientifically [18]. Therefore, exergy analysis is performed on the present IGCC system, and the exergy efficiency of each sub-system and the IGCC system are obtained to assess the difference of the IGCC system ground energy in terms of quality.

Exergy refers to the amount of energy that can be theoretically converted into useful work in any form under ambient conditions. It is necessary to calculate the various forms of exergy values of the input and output energy systems separately before performing the exergy analysis of the energy system. For a system in stable operation, its equation of balance of exergy under controlled volume conditions can be expressed as [24]:

$$\sum \left(1 - \frac{T_0}{T}\right) Q + \sum_{in} m_i ex_i = \sum_{out} m_i ex_i + W - Ex_d \quad (7)$$

where $\left(1 - \frac{T_0}{T}\right)Q$ denotes the heat radiation obtained from heat absorption by the heat source; T_0 is the ambient temperature of 298.15 K; T denotes the actual temperature; Q is the heat flow rate; W is the work done by the system; Ex_d denotes the exergy loss. ex_i denotes the exergy of the stream, including the physical exergy ex_{ph} and the chemical exergy ex_{ch} , as follows:

$$ex_{ph} = (h - h_0) - T(s - s_0) \quad (8)$$

$$ex_{ch} = \sum n_i \cdot ex_{ch,i} + RT_0 \sum n_i \cdot \ln n_i \quad (9)$$

where h and h_0 refer to the specific enthalpy of the flow under actual and ambient conditions, respectively; s and s_0 refer to the specific entropy of the flow under actual and ambient conditions. n_i is the molar fraction of a gas i in the gas mixture; R denotes the gas constant (8.314 J/(K · mol)). $ex_{ch,i}$ refers to the molar standard chemical exergy of gas i , the specific value of which is seen in Table 7.

The standard chemical exergy of coal can be calculated by the following empirical formula of the Shinzawa [26]:

$$ex_r = LHV_{coal} \left(1.0036 + 0.1365 \frac{W_H}{W_C} + 0.0308 \frac{W_O}{W_C} + 0.0104 \frac{W_S}{W_C} \right) \quad (10)$$

where W_C , W_H , W_O , and W_S are the mass fractions of the corresponding

Table 7
Standard chemical exergy of gas species [26].

| Gases | $ex_{ch,i}$ (kJ/mol) | Gases | $ex_{ch,i}$ (kJ/mol) |
|----------------|----------------------|------------------|----------------------|
| N ₂ | 0.72 | CO | 275 |
| O ₂ | 3.97 | CO ₂ | 19.97 |
| Ar | 19.97 | H ₂ O | 9.49 |
| H ₂ | 236 | CH ₄ | 831 |

elements in the coal. The above method can be used to obtain the exergy of each flow of the IGCC system, and then the exergy efficiency is calculated to evaluate the energy. The exergy efficiency of the subsystem can be expressed as:

$$\eta_{ex,i} = \frac{EX_{out,i}}{EX_{in,i}} \times 100\% \quad (11)$$

where EX_{out} is the output exergy of subsystem i . EX_{in} is the input exergy of subsystem i . The total exergy efficiency of the IGCC system is finally given by:

$$\eta_{ex} = \frac{EX_{out}}{EX_{in}} \times 100\% \quad (12)$$

where EX_{out} represents the effective output exergy of the IGCC system. EX_{in} is composed of the fuel exergy entering the system and the exergy brought in by the flows.

Accordingly, the exergy efficiency of the ASU, gasification unit, gas turbine unit and HSRG unit are 32.8%, 66.8%, 72.7%, and 77.7%, respectively. The exergy efficiency of the IGCC system is 41.8%. Fig. 12 (a) shows the results of the exergy efficiency of each sub-system and IGCC system for the full load condition. It is found that there is a certain difference between the exergy efficiency and the energy efficiency of the IGCC sub-systems with the consideration of energy quality, and the overall energy efficiency is higher than the exergy efficiency, which also indicates that the energy utilization and conversion of the system can be more accurately revealed through the analysis of the exergy efficiency.

Energy losses is the most important factor that causes efficiency reduction, which is closely related to energy efficiency. The energy consumption of each subunit is formulated as:

$$\varphi_i = \left(1 - \frac{E_{out,i}}{E_{in,i}}\right) \times 100\% \quad (13)$$

Similarly, the exergy loss of each subunit can be given by:

$$\varphi_{ex,i} = \left(1 - \frac{EX_{out,i}}{EX_{in,i}}\right) \times 100\% \quad (14)$$

Fig. 12(b) shows the energy consumption and exergy losses of each IGCC subunit. The ASU and gasification units have high energy consumption but low efficiency, which need to be further optimized to improve system efficiency. In addition, the present IGCC system with an energy efficiency of 45.7% is also higher than the conventional IGCC system (40%–45%) [15,27,28], which also verifies the high efficiency of the present IGCC system and the reliability of the developed model in

predicting the performance of the IGCC system.

4. Conclusion

This work established a model focusing on the process modelling of a 250 MW industrial-scale IGCC system. The model was well validated with the design values and experimental data in terms of the sub-systems and the whole system. The integrated model was then applied to predict the power generation of the IGCC system under different load conditions (i.e., 50%, 70%, and 100%). The efficiency of the IGCC system was then assessed by energy analysis and exergy analysis. The conclusion can be drawn below.

- 1) Via validating the simulation results with design values and experimental data, each sub-model is demonstrated to be reliable to predict the IGCC sub-systems, including the air separation unit, coal gasification and purification unit, and gas-steam combined cycle unit. The total power generation of the IGCC system under the full load condition is 262,051 kW predicted by the integrated model via encapsulating the well-validated sub-models.
- 2) The IGCC system can operate stably under wide load conditions. Increasing the load increases the amount of syngas generated and promotes the amount of work done. The power generation of the total gas turbine system under 50%, 70%, and 100% loads is 81,530 kW, 114,320 kW, and 164,547 kW. In the steam turbine unit, the low-pressure engine has the largest power generation under all load conditions, followed by the medium-pressure engine and high-pressure engine. Increasing the load from 50% to 100%, the total power generation of the IGCC system increases by 97.1%.
- 3) The energy efficiency of the ASU, gasification unit, gas turbine unit and HSRG unit are 10.9%, 61.2%, 94.7%, and 93.2%, respectively. The thermal efficiency of the IGCC system is 45.7%, which is higher than the conventional IGCC system with energy efficiency in the range of 40%–45%. The exergy efficiency of the ASU, gasification unit, gas turbine unit and HSRG unit are 32.8%, 66.8%, 72.7%, and 77.7%, respectively. The exergy efficiency of the IGCC system is 41.8%. The exergy efficiency of the IGCC system considering the energy quality is lower than the energy efficiency, which provides a more accurate assessment of the energy utilization and conversion in the system.

The present work provides a cost-effective tool for the process modelling of the IGCC system, shedding light on future optimization. For example, the air separation unit and the gasification unit have high

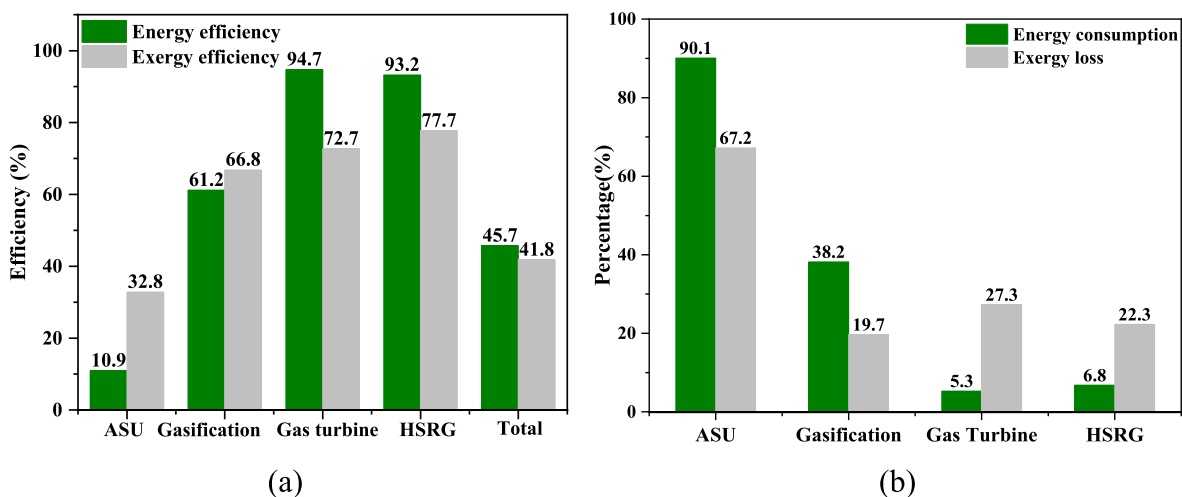


Fig. 12. Comparison of (a) energy efficiency and exergy efficiency, (b) energy consumption and exergy loss of the sub-systems and IGCC system for 100% load condition.

energy consumption but low efficiency, which needs to be further optimized to improve system efficiency.

Credit author statement

Research motivation: Kun Luo, Jianren Fan. Data post-processing: Qilong Xu, Lu Pan, Yanfei Mu. Paper writing (Draft): Qilong Xu. Paper reviewing&editing: Shuai Wang.

Declaration of competing interest

The authors declare that they have no known competing financial interests or personal relationships that could have appeared to influence the work reported in this paper.

Data availability

Data will be made available on request.

Acknowledgment

We acknowledged the support from the National Natural Science Foundation of China (No. 51925603) and the Fundamental Research Funds for the Central Universities (2022ZFJH004).

Appendix A. Supplementary data

Supplementary data to this article can be found online at <https://doi.org/10.1016/j.energy.2023.127040>.

References

- [1] Jie D, Xu X, Guo F. The future of coal supply in China based on non-fossil energy development and carbon price strategies. *Energy* 2021;220:119644.
- [2] Rahimipetroudi I, Rashid K, Yang JB, Dong SK. Development of environment-friendly dual fuel pulverized coal-natural gas combustion technology for the co-firing power plant boiler: experimental and numerical analysis. *Energy* 2021;228:120550.
- [3] Wang D, Liu D, Wang C, Zhou Y, Li X, Yang M. Flexibility improvement method of coal-fired thermal power plant based on the multi-scale utilization of steam turbine energy storage. *Energy* 2022;239:122301.
- [4] Shi Y, Zhong W, Chen X, Yu AB, Li J. Combustion optimization of ultra supercritical boiler based on artificial intelligence. *Energy* 2019;170:804–17.
- [5] Schaffel-Mancini N, Mancini M, Szlek A, Weber R. Novel conceptual design of a supercritical pulverized coal boiler utilizing high temperature air combustion (HTAC) technology. *Energy* 2010;35:2752–60.
- [6] Cocco D, Serra F, Tola V. Assessment of energy and economic benefits arising from syngas storage in IGCC power plants. *Energy* 2013;58:635–43.
- [7] Giuffrida A, Romano MC, Lozza G. Efficiency enhancement in IGCC power plants with air-blown gasification and hot gas clean-up. *Energy* 2013;53:221–9.
- [8] Zhao Y, Duan Y, Liu Q, Cui Y, Mohamed U, Zhang Y, et al. Life cycle energy-economy-environmental evaluation of coal-based CLC power plant vs. IGCC, USC and oxy-combustion power plants with/without CO₂ capture. *J Environ Chem Eng* 2021;9:106121.
- [9] Minchener AJ. Coal gasification for advanced power generation. *Fuel* 2005;84:2222–35.
- [10] Pruscek R, Oeljeklaus G, Brand V, Haupt G, Zimmermann G, Ribberink JS. Combined cycle power plant with integrated coal gasification, CO shift and CO₂ washing. *Energy Convers Manag* 1995;36:797–800.
- [11] Descamps C, Bouallou C, Kanniche M. Efficiency of an integrated gasification combined cycle (IGCC) power plant including CO₂ removal. *Energy* 2008;33:874–81.
- [12] Emun F, Gadalla M, Majazi T, Boer D. Integrated gasification combined cycle (IGCC) process simulation and optimization. *Comput Chem Eng* 2010;34:331–8.
- [13] Xie H, Zhang Z, Li Z, Wang Y. Relations among main operating parameters of gasifier in IGCC. *Energy Power Eng* 2013;5:552–6.
- [14] Nikoo MB, Mahinpey N. Simulation of biomass gasification in fluidized bed reactor using ASPEN PLUS. *Biomass Bioenergy* 2008;32:1245–54.
- [15] Lee JC, Lee HH, Joo YJ, Lee CH, Oh M. Process simulation and thermodynamic analysis of an IGCC (integrated gasification combined cycle) plant with an entrained coal gasifier. *Energy* 2014;64:58–68.
- [16] Ahmed U, Zahid U, Jeong YS, Lee C-J, Han C. IGCC process intensification for simultaneous power generation and CO₂ capture. *Chem Eng Process Process Intensif* 2016;101:72–86.
- [17] Oh H-T, Lee W-S, Ju Y, Lee C-H. Performance evaluation and carbon assessment of IGCC power plant with coal quality. *Energy* 2019;188:116063.
- [18] Giuffrida A, Romano MC, Lozza G. Thermodynamic analysis of air-blown gasification for IGCC applications. *Appl Energy* 2011;88:3949–58.
- [19] Jinghua X, Tiantian W, Mingyu G, Tao P, Shuyou Z, Jianrong T. Energy and exergy co-optimization of IGCC with lower emissions based on fuzzy supervisory predictive control. *Energy Rep* 2020;6:272–85.
- [20] Wu W, Zheng L, Shi B, Kuo P-C. Energy and exergy analysis of MSW-based IGCC power/polygeneration systems. *Energy Convers Manag* 2021;238:114119.
- [21] Lu H, Lu Y, Rostam-Abadi M. CO₂ sorbents for a sorption-enhanced water-gas-shift process in IGCC plants: a thermodynamic analysis and process simulation study. *Int J Hydrogen Energy* 2013;38:6663–72.
- [22] Seyitoglu SS, Dincer I, Kilicarslan A. Assessment of an IGCC based trigeneration system for power, hydrogen and synthesis fuel production. *Int J Hydrogen Energy* 2016;41:8168–75.
- [23] Dincer I, Rosen MA. Chapter 4 - exergy, environment, and sustainable development. In: Dincer I, Rosen MA, editors. *Exergy*. third ed. Elsevier; 2021. p. 61–89.
- [24] El-Emam RS, Dincer I, Naterer GF. Energy and exergy analyses of an integrated SOFC and coal gasification system. *Int J Hydrogen Energy* 2012;37:1689–97.
- [25] Seyitoglu SS, Dincer I, Kilicarslan A. Energy and exergy analyses of hydrogen production by coal gasification. *Int J Hydrogen Energy* 2017;42:2592–600.
- [26] Kotas TJ. *The exergy method of thermal plant analysis*. London ; Boston: Butterworths; 1985.
- [27] Chen Y-S, Hsiau S-S, Shu D-Y. System efficiency improvement of IGCC with syngas clean-up. *Energy* 2018;152:75–83.
- [28] Holt NAH. Operating experience and improvement opportunities for coal-based IGCC plants. *Mater A T High Temp* 2003;20:1–6.
- [29] Wang S, Luo K, Hu CS, Sun LY, Fan JR. Impact of operating parameters on biomass gasification in a fluidized bed reactor: An Eulerian-Lagrangian approach. *Powder Technol* 2018;333:304–16.
- [30] Wang S, Luo K, Hu CS, Lin JJ, Fan JR. CFD-DEM simulation of heat transfer in fluidized beds: Model verification, validation, and application. *Chem Eng Sci* 2019;197:280–95.
- [31] Wang S, Luo K, Fan JR. CFD-DEM coupled with thermochemical sub-models for biomass gasification: Validation and sensitivity analysis. *Chem Eng Sci* 2020;217:115550.